A hybrid method combining JFPSO and probabilistic three-phase load flow for improving unbalanced voltages in distribution systems with photovoltaic generators

F.J. Ruiz-Rodriguez, M. Gomez-Gonzalez, F. Jurado[*]

Department of Electrical Engineering, University of Jaen, 23700 EPS Linares, Jaén, Spain

[*] Corresponding author. Tel.: +34 953 648518; fax: +34 953 648586.
E-mail addresses: fjruiz@ujaen.es (F.J. Ruiz-Rodriguez), mggonzal@ujaen.es (M. Gómez-Gonzalez), fjurado@ujaen.es (F. Jurado).

Abstract

This paper presents a new hybrid method that combines JFPSO (Jumping Frog and Particle Swarm Optimization) and probabilistic three-phase load flow to improve unbalanced voltages in distribution systems with photovoltaic generators. This paper applies a new three phase probabilistic load flow based on the Monte Carlo simulation.

The voltage regulation is one of the principal problems to be addressed in photovoltaic distributed generation. The proposed method defines the nodes where PVGCS (Photovoltaic Grid-Connected System) are connected and their mean power output minimizing the maximum value of voltage unbalances at the nodes. Numerical applications are presented using the unbalanced distribution system IEEE 13-nodes and including photovoltaic generators at several nodes. The results obtained show the decrease of the unbalance factor due to the presence of distributed generation.

Keywords:

Discrete Particle Swarm Optimization, Monte Carlo method, photovoltaic systems, probabilistic load flow, three-phase load flow

Nomenclature

A	cell/module/generator surface area, m^2
BPSO	Binary Particle Swarm Optimization
CDF	cumulative distribution function
$cn_{j,k}$	customer number who belong to the *j*-th customer class for the *k*-th node of a feeder
DG	Distributed generation
GAs	Genetic Algorithms

$G_{t,\beta}(k_t, k_d)$	time averaged hourly total irradiance on a surface sloped at angle β to the horizontal, having hourly clearness index k_t, and hourly diffuse fraction k_d, W/m^2
$\mathbf{gbest}_i^{t-1}$	binary position vector that denotes the best position found for all particles of the swarm at the (t−1)-th iteration
h	hour of day, h
$\left[I_{abc}\right]_m$	Matrix of the currents in each the phases *a*, *b* and *c* in the node *m*
$\left[I_{abc}\right]_m^{line}$	Matrix of the currents in each the phases *a*, *b* and *c* in the node *m* due to line
$\left[I_{abc}\right]_m^{load}$	Matrix of the currents in each the phases *a*, *b* and *c* in the node *m* due to load
k_t	hourly clearness index ($=H_{g,h}/H_{0,h}$)
JFPSO	Jumping Frog and Particle Swarm Optimization
k_d	hourly diffuse fraction ($=H_{d,h}/H_{g,h}$)
K_T	daily clearness index ($=H_{g,d}/H_{0,d}$)
K_{Tu}	upper limit of daily clearness index
$L_j(m,h)$	TDP of the hourly active load for the *j*th customer class at *m*th month and *h*th hour, W
m	month of the year
N	number of nodes of the distribution system
n	number of simulations
ncc	number of customer classes
$\mathbf{pbest}_i^{t-1}$	binary position vector that denotes the best solution achieved for the *i*-th particle at the *(t−1)*-th iteration
p_g	constant to calculate C_g^t
p_p	constant to calculate C_p^t
$p_{w,\max}$	maximum inertial probability
$p_{w,\min}$	minimum inertial probability
PDF	probability density function
P_{pv}	DC input power to a PV inverter, W
$P_k(k_d,k_t)$	PDF of random variable hourly diffuse fraction k_d for a set of hourly events having hourly clearness index k_t
$P_K(K_T, \overline{K}_T)$	PDF of random variable daily clearness index K_T for a set of daily events having mean clearness index $\overline{K}_T$

$P\{Q\}_{L\ k}(m,h)$ hourly active {reactive} power consumed by the *k*th node of a feeder at *m*th month and *h*th hour, W{var}

PRTPLF Probabilistic radial three phase load flow

PSO Particle Swarm Optimization

PVGCS Photovoltaic Grid-Connected System

$\mathbf{rand}_i^t$ random binary position vector at the *t*-th iteration

TDPs typical daily profiles

$V_{average}$ Average value of the voltages of the three phases

V_{base} base of voltage in the system

$[V_{LGabc}]_m$ Matrix of the single phase voltages in each the phases *a, b* and *c* in node *m*

$[V_{LGabc}]_s$ Matrix of the single phase voltages in each the phases *a, b* and *c* in *source* (or *root)* node

$V_{unbalance}$ Index of unbalance of voltage

x_i Value of the variable in each simulation

$\mathbf{x}_i^{t-1}$ Binary position vector of the *i*-th particle at the (t-1)-th iteration

Y_1^t, Y_2^t and Y_3^t Inertial coefficients at the t-th iteration

Greek symbols

η_c electrical efficiency

$\mu_j(m,h)$ hourly mean value of active load for the *j*th customer class at *m*th month and *h*th hour, W

$\varsigma_{i,j}^t$ random variable that is between 0 and 1

$\sigma_j(m,h)$ hourly standard deviation of active load for the*j*th customer class at *m*th month and *h*th hour, W

Superscripts

$-$ average value

we weekend days

wo working days

1. Introduction

The electric distribution systems have unbalanced lines supplying three-phase loads [1]. These systems present voltage unbalances. The unbalance is a state of a three-phase system in which the RMS values of the line voltages, and/or the phase angles between successive line voltages, are not all equal and/or 120º displaced.

Distributed Generation (DG) is electricity generation sited close to the load it serves, typically in the same building or complex. DG creates a variety of well documented impacts on distribution network operation and implies significant changes to planning and design practices. Research has suggested that the benefits of distributed resources could be substantial. However, these distributed advantages are site specific [2-4]. A Photovoltaic Grid-Connected System (PVGCS) is chosen for DG.

To assess the unbalanced voltages of the electric distribution systems, the unavoidable uncertainties that are relevant to the information of entry of the model must be considered. The uncertainties normally are due to variations in the time of the demands of phase load, generation and topology of the system. In the last years, the new and significant causes of the uncertainties in the distribution systems are due to the distributed generation. For example, the production of energy by renewable sources - as the photovoltaic one - is powerfully associated to the uncertainties that concern the available energy of the sun.

Hence, the right valuation of the impact of renewable sources on current systems of distribution must be faced by means of a probabilistic approach [4] that also considers the unbalance of the electrical systems.

In addition, probabilistic approaches seem to be particularly useful to study in depth the influence of voltage unbalance on the performance of induction machines in stationary condition, with the objective to set up recommendations for their functioning [5]. This work studies the unbalanced three-phase systems with Photovoltaic Grid-Connected System (PVGCS). Since PVGCS have a very low efficiency (only from 8 to 15 percent of solar radiation is converted into electrical energy), it is advisable to work normally at a power factor close to the unit [6], because otherwise the PVGCS efficiency would be even lower, which would be uneconomic. If the power factor is near to the unit, reactive power generated, *Q*, is zero or very small. Therefore, it is not possible to control the voltage at the nodes. Then, the nodes with PVGCS are considered PQ, being *Q* equal to zero. The direction of the real power injected in the system from PVGCS, *P*, is opposite than that for loads. For this reason, PVGCS are mathematically considered as negative loads in the load flow.

In this work, the model of PVGCS is incorporated into the three-phase load flow equations and the Monte Carlo simulation method is used to consider the random inputs, not only the active and reactive loads, but also the distributed generation.

Using deterministic load flow analysis, it is not possible to measure with objectivity how often and where overvoltages or undervoltages happen in the network during a period of time. This can be accomplished by employing probabilistic techniques like the probabilistic load flow or the Monte Carlo simulation. Probabilistic load flow demands modeling of loads and power productions as probability density functions and supplies the complete range of all probable values for the node voltages and load flows in the study with their respective probabilities assuming generation and load uncertainties and correlations and topological changes. The probabilistic load flow was enunciated in [7], [8], and further developed at a greater extent in [9, 10].

In [11] the probabilistic power flow was extended to the three-phase field to evaluate the uncertainties which affect the steady-state operating conditions of an unbalanced power system. Both Monte Carlo procedure and a linearized form were proposed. Various distribution system load flow algorithms, based on the forward/backward sweeps, were reviewed, and their convergence ability was quantitatively evaluated for different loading conditions in [12, 13].

In [14] was presented a three-phase power flow solution method for real-time analysis of primary distribution systems. This method is a direct extension of the compensation-based power flow method for weakly meshed distribution systems from single phase to three-phase. For asymmetrical three-phase load-flow study, two methods based on symmetrical component theory, the node admittance method and the decoupling compensation method were proposed in [15].

Artificial Intelligence based methods, does not always guarantee the optimal solution, they provide near solutions to the optimal in short CPU times. Particle Swarm Optimization (PSO) is a nature-inspired evolutionary stochastic algorithm developed by Kennedy and Eberhart [16]. This technique, motivated by social behavior of organisms such as bird flocking and fish schooling, has been shown to be effective in optimizing multidimensional problems. PSO algorithm is very easy to be implemented and requires a few parameters to adjust. In this paper, a hybrid method that uses a discrete particle swarm optimization and probabilistic three-phase load flow is proposed to search a large range of combinations for location and size of single-phase photovoltaic generators that minimize the unbalance between phases. This method reduces the time of computation and it provides a good performance in comparison to Monte Carlo simulation.

2. Probabilistic PV system model

Solar irradiation on a horizontal surface inside the atmosphere cannot be predicted exactly; it depends on the irregular presence of clouds [1]. The randomness introduced by clouds on terrestrial radiation is characterized with two random variables [17,18]: the daily clearness index K_T and the hourly diffuse fraction k_d. The statistical properties of the components of solar radiation allow constructing a probability model (using PDFs and CDFs). These properties provide the probability for K_T [17] and k_d [18].

If the random variables $k_t(K_T)$ and k_d are known, then it is possible to determine the random variable $G_{t,\beta}$ as a linear combination of $k_t(K_T)$ and k_d. At this point, the Cumulant Method [19] allows a statistical information mapping of predefined random variables k_t and k_d with the new random variable $G_{t,\beta}$. If the variable $G_{t,\beta}$ is known, the power output is obtained from a linear combination of $G_{t,\beta}$once the correlations used between both variables are linearized.

2.1 Probability density function for global irradiance

Most works involving the analysis of the statistical properties of global irradiation use set of daily solar irradiation data. Holland and Huget suggested the following PDF [17]

$$P_K(K_T, \overline{K}_T) = C_1\left(1-\frac{K_T}{K_{Tu}}\right)\exp(\lambda K_T) \quad (1)$$

Where C_1 and λ are functions of K_{Tu} and $\overline{K}_T$.

2.2. Probability density function for diffuse irradiance

Using the expected value approach of probability theory Hollands [18] gave a general-purpose expression containing the PDF for k_d

$$P_k(k_d, k_t) = C_3(k_d - k_{dl})(1-k_d)\exp(\lambda k_d) \quad (2)$$

Where C_3, λ *and* k_{dl} are functions of $\overline{k}_d$.

2.3. Probability density function for PV electrical power

The PV electrical power (DC side) P_{pv} is calculated as linear function of the total irradiance on PV surface ($G_{t,\beta}$) [20, 21]:

$$P_{pv} = \eta_c A G_{t,\beta} \quad (3)$$

3. Probabilistic load model

The electric load of a power system has deterministic and stochastic components [1]. The two main deterministic factors that affect the load are: time (multiple seasonal patterns: yearly, weekly and intra-daily) and weather conditions. However, there is also a random component in load which cannot be explained, resulting from the random behavior of energy customers. Customers are classified by electric utilities into different subjective classes [22].

Typical load patterns of customer classes can be obtained from statistical analysis of historical data. Thus, reference [22] defines the TDPs for each type of customer, which contained information about daily load profile after extracting all exogenous information, i.e. seasonal (yearly and weekly cycles) and weather information. Additionally, Jardini et al. [22] apply statistical analysis methods to the TDPs, allowing to construct a probability model (using PDFs) capable of giving the probability that a value of observed load will be within specified limits. Its approach treats the TDPs of each jth customer class $L_j(m,h)$ as a random variable, normally distributed, which changed month to month and hour to hour. This means that its hourly mean value $\mu_j(m,h)$and the corresponding standard deviation $\sigma_j(m,h)$ changed throughout the 12 months and 24 hour period.

However, the seasonal information when TDPs are built is only partially extracted. Thus, for the jth customer class are built two TDPs per month, one for weekend days $L_j^{we}(m)$ and another one for working days $L_j^{wo}(m)$. The one-year TDPs are arranged into two-dimensional layout with 12 columns representing 12 month of a year and 2 rows representing weekend or working days.

Known the TDPs of customer classes it is possible to determine the random variable hourly active power consumed by the kth node of a feeder at mth month and hth hour adding the random variables individual consumptions $L_j(m,h)$ for each type of customer. For example for working days

$$P_{L\,k}^{wo}(m,h) = \sum_{j=1}^{j=ncc} cn_{j,k} L_j^{wo}(m,h) \tag{4}$$

Assuming a deterministic power factor the relevant reactive power consumed is

$$Q_{L\,k}(m,h) = P_{l\,k}(m,h) \tan\varphi \tag{5}$$

4.Probabilistic radial three phase load flow (PRTPLF)

4.1. Radial three phase load flow

The conventional method applied to the resolution of load flows is not valid for radial systems due to its poor convergence [23]. Therefore, it is advisable to use another technique which takes into account such systems.

The method is an iterative process, which finds the solution covering all the nodes of the system, first forward and backward, then backward (root node) and forward (extreme nodes). These steps are done until convergence criterion is reached. The steps are as follows:

Consider the system in the Fig. 1. The process begins by determining the current at the load node 3 with the following expression:

$$I_3 = \left(\frac{S_3}{V_3}\right)^* \tag{6}$$

Fig. 1.Example of radial system.

where S_3 is the complex power of the load node 3, and V_3 is the voltage at the node 3. For the first iteration, this voltage is equal to one of the source node.

Since in general, these systems are unbalanced, the above equation is valid for each of the phases:

$$I_{3a} = \left(\frac{S_{3a}}{V_{3a}}\right)^* ; \quad I_{3b} = \left(\frac{S_{3b}}{V_{3b}}\right)^* ; \quad I_{3c} = \left(\frac{S_{3c}}{V_{3c}}\right)^* \tag{7}$$

being a, b and c the phases of the system.

From current at the node 3, the voltage and current can be determined at the node 2. Therefore, in matrix form:

$$
\begin{aligned}
\left[V_{LGabc}\right]_2 &= [a]\cdot\left[V_{LGabc}\right]_3 + [b]\cdot\left[I_{abc}\right]_3 \\
\left[I_{abc}\right]_2^{line} &= [c]\cdot\left[V_{LGabc}\right]_3 + [d]\cdot\left[I_{abc}\right]_3
\end{aligned}
\tag{8}
$$

The matrices of coefficients *a*, *b*, *c* and *d*, are determined as stated in [24]. System configurations (unbalanced and single-phase lines, neutral conductors and groundings, etc.) have taken into account these matrices of coefficients.

From voltage at the node 2, it is possible to obtain the current due to the load conditions at this node by the equations (7) $\left[I_{abc}\right]_2^{load}$. Therefore the total current can be determined per phase in the node 2 as:

$$
\left[I_{abc}\right]_2 = \left[I_{abc}\right]_2^{load} + \left[I_{abc}\right]_2^{line}
\tag{9}
$$

Again, by the equations (8), the voltages and currents per phase can be obtained at the source node (node 1), $\left[V_{LGabc}\right]_1, \left[I_{abc}\right]_1$.

At this point, the convergence criterion is applied:

$$
[Mismatches] = \frac{\left|\left[V_{LGabc}\right]_s - \left[V_{LGabc}\right]_1\right|}{V_{base}}
\tag{10}
$$

If all the errors in each element of vector [*Mismatches*] are less than 0.001 p.u., the solution is considered valid. Otherwise, the process continues with the next step (backward sweep).

In this step, the reference voltage $\left[V_{LGabc}\right]_s$ is considered at node 1. The voltages at the successive nodes are calculated, regarding the currents calculated above, by the following expressions:

$$
\begin{aligned}
\left[V_{LGabc}\right]_2 &= [A_1]\cdot\left[V_{LGabc}\right]_s - [B_1]\cdot\left[I_{abc}\right]_2 \\
\left[V_{LGabc}\right]_3 &= [A_2]\cdot\left[V_{LGabc}\right]_2 - [B_2]\cdot\left[I_{abc}\right]_3
\end{aligned}
\tag{11}
$$

where the matrices $\left[A_1\right],\left[B_1\right],\left[A_2\right],\left[B_2\right]$ are calculated according to [24].

With these new voltages, the method turns to perform step 1. This whole process will be held until that convergence criterion is reached. In this process, the photovoltaic generators are treated as negative loads [6].

The index of unbalance of voltage at each node is defined as [24]:

$$V_{unbalance}(\%) = \frac{\left|\text{Maximum deviation from average}\right|}{\left|V_{average}\right|}\cdot 100 \qquad (12)$$

4.2. Simulation method

This technique is basically to select values of input variables randomly from their distribution functions, and with these values to solve a deterministic radial three phase load flow (Fig. 2). After a certain number of simulations, the probabilistic solution of the problem is reconstructed from deterministic data obtained for each simulation.

It is worthy that the number of simulations needed to obtain a sufficiently precise result using Monte Carlo method is independent of system size [25]. The number of simulations that has been estimated as adequate for this problem and has also been used in several articles to solve probabilistic load flow is 10000 [26, 27].

Fig. 2. Flow-chart of the Monte Carlo simulation.

The mean is determined by the following equation:

$$\bar{x} = \sum_{i=1}^{n} \frac{x_i}{n} \qquad (13)$$

The typical deviation is set by the equation:

$$\sigma = \sqrt{\sum_{i=1}^{n} \frac{\left(x_i - \bar{x}\right)^2}{(n-1)}} \qquad (14)$$

5. Particle Swarm Optimization

5.1. Discrete Particle Swarm Optimization

The underlying principle of the traditional PSO is that the next position of each particle is a compromise of its current position, the best position in its history so far, and the best position among all existing particles. In order to solve optimization problems in discrete search spaces, Kennedy and Eberhart in 1997 [16] developed a binary version of PSO (Standard BPSO). In this version, the position of each particle is a binary vector in the L-dimensional binary space, $\mathbf{x}_i^t = [x_{i,1}^t, x_{i,2}^t, ..., x_{i,L}^t]$, but the velocity is still a L-dimensional vector of the continuous L-dimensional space, $\mathbf{v}_i^t = [v_{i,1}^t, v_{i,2}^t, ..., v_{i,L}^t]$. The velocity is also interpreted as the rate of change for each component of the position vector and is updated by:

$$\mathbf{v}_i^t = w \cdot \mathbf{v}_i^{t-1} + c_1 \cdot \mathbf{rand}_{1,i}^t (\mathbf{pbest}_i^{t-1} - \mathbf{x}_i^{t-1}) + c_2 \cdot \mathbf{rand}_{2,i}^t (\mathbf{gbest}_i^{t-1} - \mathbf{x}_i^{t-1}) \tag{15}$$

$$\mathbf{x}_i^t = \mathbf{x}_i^{t-1} + \mathbf{v}_i^t \tag{16}$$

Where $c_1$is the cognition learning factor, c_2 is the social learning factor, w is the inertia weight, $\mathbf{rand}\mathit{1}_i^t = [rand1_{i,1}^t, rand1_{i,2}^t, ..., rand1_{i,L}^t]$ and $\mathbf{rand2}_i^t = [rand2_{i,1}^t, rand2_{i,2}^t, ..., rand2_{i,L}^t]$are random L-length binary strings, whose components are ’0’ or ’1’ with the same probability; $\mathbf{x}_i^{t-1} = [x_{i,1}^{t-1}, x_{i,2}^{t-1}, ..., x_{i,L}^{t-1}]$, denotes the binary position vector of the i-th particle at the (t-1)-th iteration; $\mathbf{pbest}_i^{t-1} = [pbest_{i,1}^{t-1}, pbest_{i,2}^{t-1}, ..., pbest_{i,L}^{t-1}]$ is the best solution achieved for the i-th particle at the (t−1)-th iteration and $\mathbf{gbest}_i^{t-1} = [gbest_1^{t-1}, gbest_2^{t-1}, ..., gbest_L^{t-1}]$ is the best position found for all particles in the swarm at the (t−1)-th iteration. $\mathbf{pbest}_i^{t-1}$, $\mathbf{gbest}_i^{t-1}$and $\mathbf{x}_i^{t-1}$ are L-length binary string.

Nevertheless, the position is obtained solely from the velocity by a new procedure. The original proposal by the authors of the PSO uses the sigmoid function. Then, every variable x_{ij} of the particles takes value 1 with probability $(1 + \exp(-v_{ij}))^{-1}$, and 0 otherwise.

The changes of velocity are in terms of probabilities by encoding the particle's position as a binary vector and using a stochastic velocity scheme. Other versions of discrete particle swarm optimization have been introduced for example in [28-33].

5.2. Jumping Frog Optimization

The Jumping Frog Optimization (JFO) approach proposed in [34, 35] is based on the particles point of view instead of the solutions or particle's position. JFO is inspired in the behavior of a group of frogs looking around for food while jumping from lily pad to lily pad. This group of frogs competes for food by jumping to the best locations so that if a frog is well-placed, then other frogs tend to move towards it. The JFO approach uses an interesting scheme without the need of velocity to update the particle's position. Instead, the position is updated using a follower-attractor system. When a particle wants to jump to a new better position, the particle uses a better positioned particle as a reference. The equation updates the particle's position is:

$$\mathbf{x}_i^t = c_1 \cdot \mathbf{x}_i \oplus c_2 \cdot \mathbf{pbest}_i^{t-1} \oplus c_3 \cdot \mathbf{gbest}_i^{t-1} \quad (17)$$

The algorithm interprets the weights of the equation (17) as the probability for a behavior at random, or guided by attraction to the best position for the individual particle, or by attraction of the best global position. This results random moves with probability c_1, approaching moves towards the best position of the individual particle with probability c_2, or towards the best global position with probability c_3.

5.3. Proposed algorithm: JFPSO

This paper aims at creating a novel discrete PSO, denominated JFPSO, in which each particle is a string of binary numbers, whose components are '0' or '1'. The proposed algorithm is based on the following equation:

$$\mathbf{x}_i^t = \mathbf{rand}_i^t \oplus \mathbf{pbest}_i^{t-1} \oplus \mathbf{gbest}_i^{t-1} \oplus \mathbf{x}_i^{t-1} \quad (18)$$

Where $\mathbf{rand}_i^t = [rand_{i,1}^t, rand_{i,2}^t, ..., rand_{i,L}^t]$ is a random L-length binary string, whose components are '0' or '1' with the same probability, $\mathbf{x}_i^{t-1} = [x_{i,1}^{t-1}, x_{i,2}^{t-1}, ..., x_{i,L}^{t-1}]$, denotes the binary position vector of the i-th particle at the (t-1)-th iteration,

$\mathbf{pbest}_i^{t-1} = [pbest_{i,1}^{t-1}, pbest_{i,2}^{t-1}, ..., pbest_{i,L}^{t-1}]$ is the best solution achieved for the i-th particle at the (t−1)-th iteration and $\mathbf{gbest}_i^{t-1} = [gbest_1^{t-1}, gbest_2^{t-1}, ..., gbest_L^{t-1}]$ is the best position found for all particles in the swarm at the (t−1)-th iteration. $\mathbf{pbest}_i^{t-1}$, $\mathbf{gbest}_i^{t-1}$ and $\mathbf{x}_i^{t-1}$ are L-length binary string. Every bit $x_{i,j}^t$ is calculated:

$$\begin{aligned} &\text{If } \left(0 \le \varsigma_{i,j}^t < Y_1^t\right) \Rightarrow x_{i,j}^t = rand_{i,j}^t \\ &\text{else if } \left(Y_1^t \le \varsigma_{i,j}^t < Y_2^t\right) \Rightarrow x_{i,j}^t = pbest_{i,j}^{t-1} \\ &\text{else if } \left(Y_2^t \le \varsigma_{i,j}^t < Y_3^t\right) \Rightarrow x_{i,j}^t = gbest_{i,j}^{t-1} \\ &\text{else } \left(Y_3^t \le \varsigma_{i,j}^t \le 1\right) \Rightarrow x_{i,j}^t = x_{i,j}^{t-1} \end{aligned} \tag{19}$$

Where $\varsigma_{i,j}^t$ is a random variable, its value is between 0 and 1.

In order to provide exploration at the first iterations and more exploitation at the last iterations, the inertial coefficients Y_1^t, Y_2^t and Y_3^t are defined in the followings equations:

$$Y_1^t = p_{\omega,\max} - \frac{(t-1)\cdot(p_{\omega,\max} - p_{\omega,\min})}{(t_{\max}-1)} \qquad t = 1, 2, ..., t_{\max} \tag{20}$$

$$Y_2^t = Y_1^t + (1 - Y_1^t)\cdot p_p \tag{21}$$

$$Y_3^t = Y_2^t + (1 - Y_1^t)\cdot p_g \tag{22}$$

Where $p_{w,\max}$, $p_{w,\min}$, p_p and p_g are positive constants which define the ratio between the inertial coefficients. In order to establish their values, it must meet the following: $0 < p_{w,\max} < 1$; $0 < p_p < 0.5$ and $p_p = p_g$.

Y_1^t, Y_2^t and Y_3^t evolve at each iteration. Y_1^t is calculated by means of a lineally decreasing function. Therefore, the values of Y_2^t and Y_3^t are increased with the iterations.

When t = 1: $Y_1^t = p_{w,\max}$, that represents the initial weight of $\mathbf{rand}_i^t$ on the equation (15).

When 1<t<t_{max}: Y_1^t, that represents the weight of $\mathbf{rand}_i^t$ and $(1-Y_1^t)\cdot p_p$ and $(1-Y_1^t)\cdot p_g$, that indicates the weight of the $\mathbf{pbest}_i^{t-1}$ and $\mathbf{gbest}_i^{t-1}$, respectively. The weight of $\mathbf{x}_i^{t-1}$ is $(1-Y_1^t)\cdot(1-p_p-p_g)$.

When $t = t_{max}$: $Y_1^t = p_{w,\min}$, that shows the final weight of $\mathbf{rand}_i^t$.

Thus the interval $\left(0,Y_1^t\right)$ is greater at the first iterations but decreases lineally. On the other hand, the intervals $\left(Y_1^t,Y_2^t\right)$, $\left(Y_2^t,Y_3^t\right)$ and $\left(Y_3^t,1\right)$ are increased with the advance at the algorithm.

The update process of a particle in the iteration t is the following:

1. Calculate Y_1^t from t, $p_{w,\max}$, $p_{w,\min}$ and $t_{\max}$.
2. Calculate Y_2^t and Y_3^t.
3. Calculate $x_{i,j}^t$ in according to equation (19).

Unlike PSO, the proposed JFPSO does not need to use the velocity. After Y_1, Y_2 and Y_3 are given, the proposed algorithm only uses one string **rand**, three multiplications, and one comparison. Therefore, the proposed algorithm is more efficient that PSO since the computational cost is lower. Fig.3 shows the computational flow chart of the proposed JFPSO algorithm:

Fig. 3. Flow-chart of the proposed JFPSO algorithm.

6. The proposed hybrid method JFPSO- PRTPLF

The proposed method must define the nodes where PVGCS are connected and their mean power output minimizing the maximum value of voltage unbalances at the nodes. For this reason, the chosen objective function to minimize is:

$$F = \min[\max(V_{unbalance,i})] \qquad for\ i=1, 2, 3, \ldots, N \tag{23}$$

where N = Number of nodes of the distribution system.

The proposed method consists in a JFPSO which integrates PRTPLF to calculate the objective function defined in (23). Thus JFPSO generates combinations of locations available in the network and values of mean power.

In other words, the proposed method aims to calculate the voltage unbalance in each of the nodes and select the maximum unbalance among all nodes and for each particle (locations and values of mean power). Next, it selects at each iteration the solution which presents a lower unbalance for each particle, $\mathbf{pbest}_i^t$, and the set of particles, $\mathbf{gbest}_i^t$, composing the population. Finally, the best solution in the last iteration is $\mathbf{gbest}_i^t$.

A particle is composed for L-length binary string which is divided in various sub-strings. The binary sub-strings represent as the nodes of connection as the mean power output of every PVGCS. For each particle a PRTPLF is performed which generates a value of the objective function selected.

The method should deliver the best locations, as well as the capacities available for a specified number of PVGCS. Compliance with limits associated to technical constraints is an underlying objective for distributed generation systems, which requires a particular attention. The best solution can be found in terms of other objectives, but if this solution violates the technical constraints of the distributed generation system, it might not be feasible. Fig.4 shows the computational flow chart of the proposed method JFPSO-PRTPLF:

Fig. 4. Flow-chart of the proposed method JFPSO- PRTPLF.

The entire method has been implemented in MATLAB R2012b computing environment with Core i5, 2.80 GHz computer with 4.00 GB RAM.

7. Simulation Results

7.1. Case study

For the study of the proposed method, the IEEE-13 node test feeder system has been modified [36], as shown in the Fig. 5:

Fig. 5. System used in case study.

Data of this the system are those that appear in [36], with the following caveats: 1) All loads have been considered constant PQ; 2) The load distributed between node 632 and node 671 has been eliminated; 3) Line 633-634 has been eliminated. 4) The voltage regulator in the node 650 has been deleted; 5) Line 671-692 is 100 feet length. System loads, modeled with normal random variables, are shown in Table 1.

Table 1. Loads of the system.

First, the distribution system has been simulated without distributed generation. The distribution functions of the voltage and voltage unbalance at each node has been determined. A previous study was presented not using optimization method in [1].

A series of simulations were run to define the optimal connection points and capacities for sets of 9 PVGCS. Given the 33 possible sites and the 4 possible levels of expected power output for every PVGCS (100, 200, 300 or 400 kW), P_{gi}, these represent a search space of 5.6×10^{13} combinations. Each simulation is a fairly lengthy process, but the duration is reasonable, given the strategic nature of the process. The population size and the number of generations have been selected to guarantee the convergence of the algorithms to a satisfactory solution.

As JFPSO is a relatively new algorithm, there is no theoretical basis for adjusting the parameters. This work has resorted to experiments. Extensive experiments need to be conducted with different adjusts of parameters to balance efficiency, exploration and exploitation. In this paper, the best values for the aforementioned parameters are obtained by running JFPSO algorithm 100 times. Thus, the values of the JFPSO constant parameters are: $p_{w,\max} = 0.5$, $p_{w,\min} = 0.01$, $p_p = 0.4$ and $p_g = 0.4$.

Distributed generation has been connected in some nodes, optimizing the power and location of the generators in order to the average of voltage unbalance at any node is less than 2.5%, considering that the generators are operating on a working day in summer (July), since solar radiation is abundant at this time, and the results have been compared with the previous case.

7.2. Results

The proposed work has been implemented in MATLAB R2012b computing environment with Core i5, 2.80 GHz computer with 4.00 GB RAM.

Table 2 shows the best solution achieved (location and average real power) using the hybrid method explained in Section 6, in order to the voltage unbalance at all nodes is less than 2.5%.

Table 2. Best solution achieved (location and average power of connected PVGCS).

The power of each generator is characterized through a probability density function, according to Section 2, whose first seven cumulants are shown in Table 3, in per unit, considering a base of 100MVA:

Table 3. Cumulants of the generators (p.u.).

Fig. 6 shows the form of the probability density function of the real power of these generators. The PDF for a 100 kW average power generator has been represented in this figure.

Fig. 6. PDF of a generator.

Table 4 shows the mean value of the voltages of the three phases at some nodes of the system without and with distributed generation.

Table 4. Voltages at nodes of the system.

As shown in this table, voltages at node 650 form a balanced system. However, in the rest of the system, the voltages are unbalanced.

Unacceptably low voltages can be observed when there isn't distributed generation in the system, while the voltages at these nodes improve after connecting the photovoltaic generators.

Table 5 shows the mean in per cent and standard deviation of the unbalance of voltage in each node, before and after to connecting the distributed generation.

Table 5. Unbalances among phases.

The objective function, in other words, the maximum value of unbalance of voltage at all the nodes when PVGCS are not connected, defined in eq. (12), is 11.3386 % and 1.112 is the standard deviation. It can be seen how without DG at nodes 671, 611, 684, 692, 675, 652 and 680, the voltage unbalances are inadmissible for the proper functioning of the system. When DG is connected these voltage unbalances are improved.

In Fig. 7 can be seen the CDF for the voltage unbalance at node 633 without and with DG.

Fig. 7. CDF of the voltage unbalance at node 633.

Fig. 8 shows the voltage unbalance profiles of the system, from their mean values, before and after to connecting the DG. The objective function involves the placing of PV generators, so that the mean of unbalanced voltages at all nodes of the system does not exceed 2.5%. So, the voltage unbalances at some nodes (646 and 645) can increase with DG, but these unbalances will always be lower than 2.5%.

Fig. 8. Voltages unbalance profiles.

It can be seen in figures 7 and 8 how the voltage unbalances at the nodes have decreased considerably after the connection of the distributed generation.

From the CDFs for the voltage unbalances it can be determined the probability that the value of unbalance does not exceed a specified limit. Table 6 shows the probability that the unbalance of each node is less than 2.5 per cent, for the system with DG.

Table 6. Probability of unbalanced voltages lower to 2.5 per cent.

Comparative results between the proposed JFPSO algorithm, Standard BPSO and Genetic Algorithms (GAs). With the aim to perform a fair comparison among the chosen metaheuristics, the number of evaluations of the fitness function must be similar in all approaches. In Table 7 are shown the data used in the simulations with JFPSO, Standard BPSO and GAs. In Table 8 are presented the results obtained for each method after 30 runs.

Table 7. Data used in the simulations with JFPSO, Standard BPSO and GAs

Table 8. Results for Proposed JFPSO, Standard BPSO and GAs

Table 8 indicates that the computation time for the algorithm used is about $7 \cdot 10^3$ s. On the other hand, by an exhaustive search method the computation time is estimated about $2{,}5 \cdot 10^{14}$ s, which means $3{,}6 \cdot 10^{10}$ times more than using metaheuristic techniques.

Finally, Fig. 9 shows and compares the convergence curves of the objective function according to iterations, for all the algorithms used, the proposed JFPSO, Standard BPSO and GAs.

Fig. 9. Convergence curves of the used algorithms.

Table 8 and Fig. 9 show that the proposed JFPSO algorithm presents the best results. The algorithm converges before the other methods converge, and is more efficient, robust, and accurate. JFPSO presents an excellent capacity of exploration in complex search space and the intensification is very high. The compromise achieved between diversification (exploration) and intensification (exploitation) is higher than that with GAs and Standard BPSO.

BPSO and GAs algorithms converge to solutions of lower quality than those obtained by the proposed JFPSO. These algorithms reach good solutions, but to obtain the results from JFPSO, are necessary more evaluations. Hence, this increasing the number of particles and/or iterations, and then the computational cost will be higher.

8. Conclusions

This paper has presented a new hybrid method that combines JFPSO and probabilistic three-phase load flow to improve unbalanced voltages in distribution systems with photovoltaic generators. This paper has applied a new three phase probabilistic load flow based on the Monte Carlo simulation.

To evaluate the performance of photovoltaic system a probabilistic model is used. The probabilistic analysis has permitted the consideration of the uncertainties associated with the active and reactive loads and the solar radiation. Therefore, loads and distributed generation production have been modeled as random variables. The proposed method has defined the nodes where PVGCS are connected and their mean power output minimizing the maximum value of voltage unbalances at the nodes.

Results have proved that the proposed method can be applied for the keeping of voltages within desired limits at all load nodes of a photovoltaic grid-connected system. In addition, the probability of unbalance at the nodes has been decreased considerably.

Numerical applications have been showed and discoursed with reference to the IEEE-13 node test feeder system including PVGCS at several nodes. The results obtained have shown the decrease of the unbalance factor due to the distributed generation.

The simulation results have demonstrated the good performance of the proposed method in comparison with GAs and BPSO. Acceptable solutions have been reached in smaller number of iterations. Therefore, convergence is quickly reached and computational cost is low enough than that required for GAs, BPSO and obviously the exhaustive search methods.

REFERENCES

[1] Ruiz-Rodriguez FJ, Jurado F, Kamel S (2012) Application of probabilistic three-phase load flow for electrical distribution systems with photovoltaic generators. Przegląd Elektrotechniczny 88(7A):38-42.

[2] Nara K, Hayashi Y, Ikeda K, Ashizawa T (2001) Application of tabu search to optimal placement of distributed generators. Proceedings of the IEEE PES 2(Winter Meeting):918-923.

[3] Celli G, Ghiani E, Mocci S, Pilo F (2005) A multiobjective evolutionary algorithm for the sizing and siting of distributed generation. IEEE Transactions on Power Systems 20(2):750-757.

[4] Caramia P, Carpinelli G, Pagano M, Varilone P (2007) Probabilistic three-phase load flow for unbalanced electrical distribution systems with wind farms. IET Renewable Power Generation 1(2):115-122.

[5] Faiz J, Ebrahimpour H (2005) Precise derating of three-phase induction motors with unbalanced voltages. Conference Record - IAS Annual Meeting (IEEE Industry Applications Society) 1:485-491.

[6] Hernandez JC, Medina A, Jurado F (2006) Optimal allocation and sizing for profitability and voltage enhancement of PV systems on feeders. Renewable Energy 32(10):1768-1789.

[7] Borkowska B (1974) Probabilistic load flow. IEEE Trans Power Appar Syst PAS-93(3):752–759.

[8] Allan ......ml++RN, Borkowska B, Grigg CH (1974) Probabilistic analysis of power flows. Proc. IEE 121(12):1551–1555.

[9] Allan RN, Leite da Silva AM (1981) Probabilistic load flow using multilinearisations. Proc. IEE 128(5):280–287.

[10] Leite da Silva AM, Allan RN, Soares SM, Arienti VL (1985) Probabilistic load flow considering network outages. Proc IEE 132(3):139–145.

[11] Caramia P, Carpinelli G, Varilone P, Varilone P, Verde P (1999) Probabilistic three-phase load flow. International Journal of Electrical Power & Energy Systems 21(1):55-69.

[12] Eminoglu U, Hocaoglu MH (2009) Distribution Systems Forward/Backward Sweep-based Power Flow Algorithms: A Review and Comparison Study. Electric Power Components and Systems 37(1):91-110.

[13] Augugliaro A, Dusonchet L, Favuzza S (2008) A new backward/forward method for solving radial distribution networks with PV nodes. Electric Power Systems Research 78(3):330-336.

[14] Cheng CS, Shirmohammadi D (1995) A 3-Phase power-flow method for real-time distribution-system analysis. IEEE Transactions on Power Systems 10(2):671-678.

[15] Zhang XP, Chen H (1994) Asymmetrical 3-Phase Load-Flow Study Based On Symmetrical Component Theory. IEE Proceedings-Generation Transmission and Distribution 141(3):248-252.

[16] Kennedy J, Eberhart RC (1997) A discrete binary version of the particle swarm algorithm. Proceedings of IEEE Conference on Systems, Man and Cybernetics 5:4104-4108.

[17] Hollands KGT, Huget RG (1983) A probability density function for the clearness index, with applications. Solar Energy 30(3):195–209.

[18] Hollands KGT, Crha SJ (1987) A probability density function for the diffuse fraction, with applications. Solar Energy 38(4):237–245.

[19] Papoulis A, Pillai S (2002) Probability, Random Variables, and Stochastic Processes, 4th ed. McGraw-Hill, New York.

[20] Ruiz-Rodriguez FJ, Gomez-Gonzalez M, Jurado F (2011) Binary particle swarm optimization for optimization of photovoltaic generators in radial distribution systems using probabilistic load flow. Electric Power Components and Systems 39(15): 1667-1684.

[21] Ruiz-Rodriguez FJ, Hernandez JC, Jurado F (2012) Probabilistic load flow for radial distribution networks with photovoltaic generators. IET Renewable Power Generation 6(2):110-121.

[22] Jardini JA, Tahan CMV, Gouvea MR, Ahn SU, Figueiredo, FM (2000) Daily load profiles for residential, commercial industrial low voltage consumers. IEEE Transactions on Power Delivery 15(1):375–380.

[23] Shirmohammamdi D, Hong HW, Semlyen A, Luo GX (1988) A compensation-based power flow method for weakly Meshed distribution and transmission network. IEEE Transactions on Power Systems 3(2): 753-762.

[24] Kersting WH (2012) Distribution System Modeling and Analysis, 3rd ed. CRC Press, New Mexico.

[25] Anders GJ (1990) Probability Concepts in Electric Power Systems. John Wiley and Sons, New York.

[26] Meliopoulos APS, Cokkinides GJ, Yong Chao X (1990) A new probabilistic power flow analysis method. IEEE Transactions on Power Systems 5(1):182-190.

[27] Allan RN, Leite da Silva AM, Burchett RC (1981) Evaluation methods and accuracy in probabilistic load flow solutions. IEEE Transactions on Power Apparatus and Systems PAS-100(5):2539-2546.

[28] Lopez PR, Gonzalez MG, Reyes NR, Jurado F (2008) Optimization of biomass fuelled systems for distributed power generation using Particle Swarm Optimization. Electric Power System Research 78(8):1448-1455.

[29] Gómez M, López A, Jurado F (2010) Optimal placement and sizing from standpoint of the investor of photovoltaics grid-connected systems using binary particle swarm optimization. Applied Energy 87(6):1911-1918.

[30] Gómez M, Jurado F, Díaz P, Ruiz-Reyes N (2010) Evaluation of a particle swarm optimization based method for optimal location of photovoltaic grid-connected systems. Electric Power Components and Systems 38(10):1123-1138.

[31] Gómez-González M, Jurado F (2011) A binary shuffled frog-leaping algorithm for the optimal placement and sizing of photovoltaics grid-connected systems. International Review of Electrical Engineering 6(1):452-458.

[32] Gomez-Gonzalez M, Ruiz-Rodriguez FJ, Jurado F (2013) A binary SFLA for probabilistic three-phase load flow in unbalanced distribution systems with technical constraints. International Journal of Electrical Power and Energy Systems 48(1):48-57.

[33] Ruiz-Rodriguez FJ, Gomez-Gonzalez M, and Jurado F (2013) Optimization of radial systems with biomass fueled gas engine from a metaheuristic and probabilistic point of view. Energy Conversion and Management 65:343-350.

[34] Martinez FJ, Moreno JA (2008) Jumping Frogs Optimization: a New Swarm Method for Discrete Optimization. University of La Laguna, Tenerife.

[35] Martinez FJ, Moreno JA (2007) Discrete particle swarm optimization for the p-median problem. Metaheuristics International Conference 1-6.

[36] Kersting WH (2010) Radial Distribution Test Feeders. Distribution System Analysis Subcommittee
Available:http://www.ewh.ieee.org/soc/pes/dsacom/testfeeders/index.html

List of tables and figures

Table 1. Loads of the system.

	Phase a		Phase b		Phase c		
Node	kW	KVAr	kW	KVAr	kW	kVAr	Deviation
646			230	132			0.07
645			170	125			0.06
671	385	220	385	220	385	220	0.10
611					170	80	0.04
692					170	151	0.07
675	485	190	68	60	290	212	0.06
652	128	86					0.04

Table 2. Best solution achieved (location and average power of connected PVGCS).

Node	Phase a (kW)	Phase b (kW)	Phase c (kW)
646		400	
645		100	
671	200		
611			200
692	200		
675	200		400
680	300		100

Table 3. Cumulants of the generators (p.u.).

k_1	0,001	0,002	0,003	0,004
k_2	5,774e-08	2,309e-07	5,197e-07	9,239e-07
k_3	-1,573e-11	-1,258e-10	-4,247e-10	-1,006e-09
k_4	4,159e-15	6,655e-14	3,369e-13	1,064e-12
k_5	2,272e-19	7,271e-18	5,521e-17	2,326e-16
k_6	-1,899e-21	-1,215e-19	-1,385e-18	-7,781e-18
k_7	1,966e-24	2,516e-22	4,299e-21	3,221e-20

Table 4. Voltages at nodes of the system.

Node/ Phase	Without DG			With DG		
	Voltage (p.u.)	Deviation	Angle (º)	Voltage (p.u.)	Deviation	Angle (º)
V650a	1.0199	6.36e-07	7.07e-05	1.0200	1.68e-06	3.89e-05
V650b	1.0199	1.00e-06	-120.001	1.0199	2.82e-06	-120.001
V650c	1.0199	2.21e-06	120.001	1.0199	3.74e-06	120.001
V646a	0.9932	0.0028	-2.1772	1.0080	0.0073	0.2536
V646b	0.9879	0.0026	-121.66	0.9929	0.0118	-120.12
V646c	0.9802	0.0031	117.72	1.0001	0.0072	119.01
V633a	0.9932	0.0028	-2.1772	1.0080	0.0073	0.2536
V633b	1.0073	0.0022	-121.40	0.9969	0.0069	-120.76
V633c	0.9754	0.0031	117.85	1.0012	0.0075	119.18
V684a	0.9698	0.0057	-5.4539	0.9847	0.0154	0.2409
V684b	1.0219	0.0041	-121.57	0.9907	0.0074	-122.15
V684c	0.9178	0.0065	115.70	0.9838	0.0157	118.81
V675a	0.9650	0.0061	-5.8028	0.9827	0.0157	0.1578
V675b	1.0255	0.0040	-121.72	0.9923	0.0071	-122.39
V675c	0.9162	0.0065	115.802	0.9854	0.0167	118.91
V680a	0.9718	0.0057	-5.4251	0.9896	0.0171	0.8188
V680b	1.0219	0.0041	-121.57	0.9867	0.0081	-122.28
V680c	0.9202	0.0064	115.81	0.9872	0.0152	118.75

Table 5. Unbalances among phases.

Node	Without DG		With DG	
	Mean value (%)	Deviation	Mean value (%)	Deviation
650	0.0039	0.0001	0.0041	0.0003
632	3.2447	0.5525	1.5613	0.7955
646	1.4305	0.5606	1.9322	0.9663
645	1.6824	0.5477	1.8979	0.9255
633	3.2450	0.5525	1.5614	0.7956
671	10.5264	1.090	2.3439	1.3226
611	11.0448	1.100	2.3890	1.3304
684	10.7900	1.095	2.3775	1.3287
692	10.8190	1.098	2.4007	1.3558
675	11.3386	1.112	2.4845	1.4074
652	10.8119	1.097	2.4904	1.3853
680	10.5264	1.090	2.3731	1.3090

Table 6.Probability of unbalanced voltages lower to 2.5 per cent.

Node	**Probability (%)**
650	99.99
632	87.20
646	74.41
645	75.46
633	87.22
671	61.83
611	59.59
684	59.99
692	58.83
675	55.85
652	55.39
680	59.31

Table 7. Data used in the simulations with JFPSO, Standard BPSO and GAs

SIMULATIONS DATA – JFPSO	
Population size	30
Iterations, t_{max}	50
$p_{w,\max}$	0.5
$p_{w,\min}$	0.01
p_p	0.4
p_g	0.4
SIMULATIONS DATA – StdBPSO	
Population size	30
Iterations	50
Acceleration factors	2
Inertia weight	1.0
SIMULATIONS DATA – GAs	
Population size	38
Iterations	50
Crossover rate	0.8
Mutation rate	0.05

Table 8. Results for proposed JFPSO, Standard BPSO and GAs

Simulation	Method	Objective Function Mean Value	Objective Function Optimun Value	Standard Deviation	CPU Time
9 PVGCS	**JFPSO**	**2.3928**	**2.2949**	**0.1095**	**6792 s.**
	StdBPSO	2.7569	2.4845	0.2088	6883 s.
	GAs	2.9482	2.6604	0.2380	7226 s.

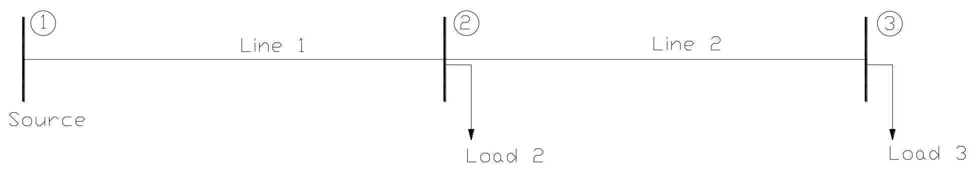

Fig. 1.Example of radial system.

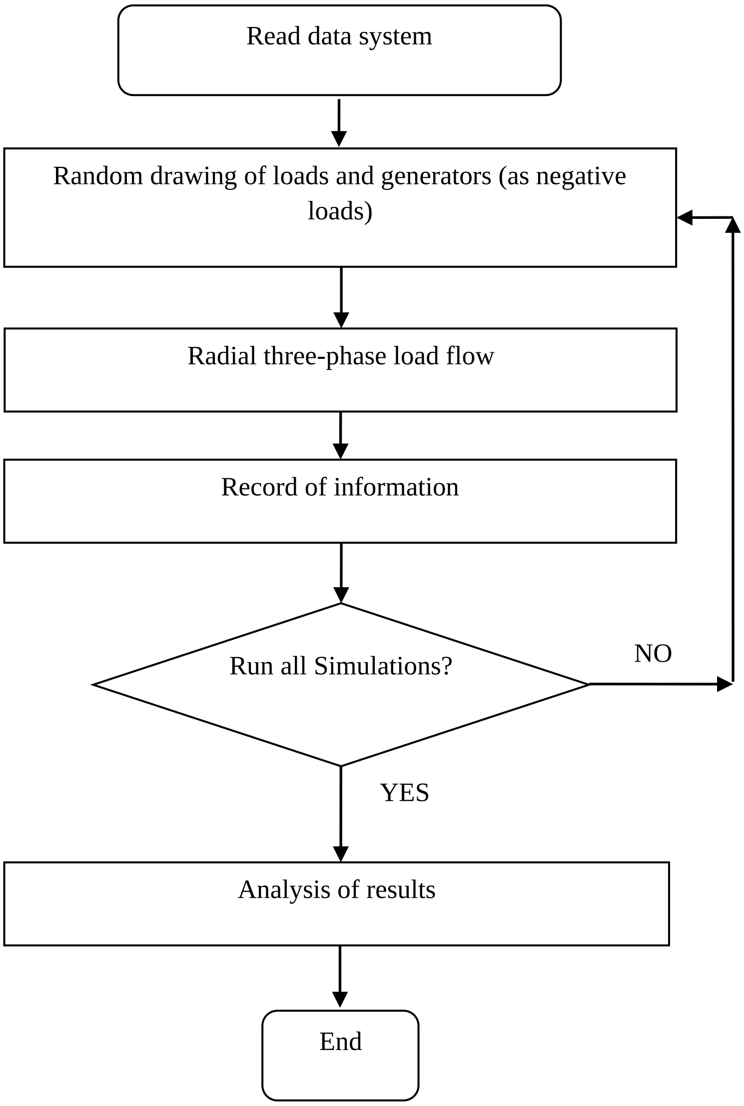

Fig. 2. Flow-chart of the Monte Carlo simulation.

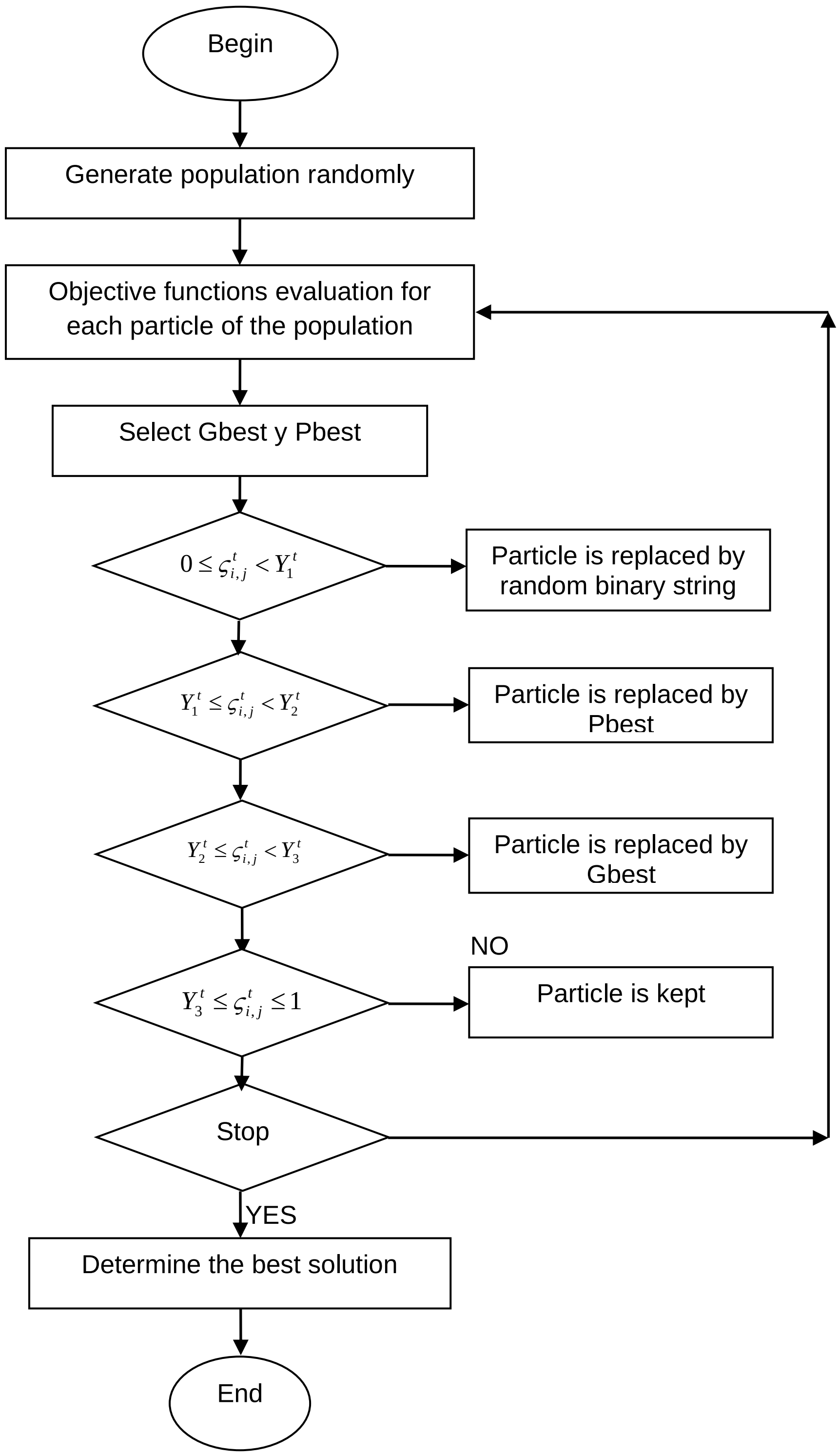

Fig. 3. Flow-chart of the proposed JFPSO algorithm.

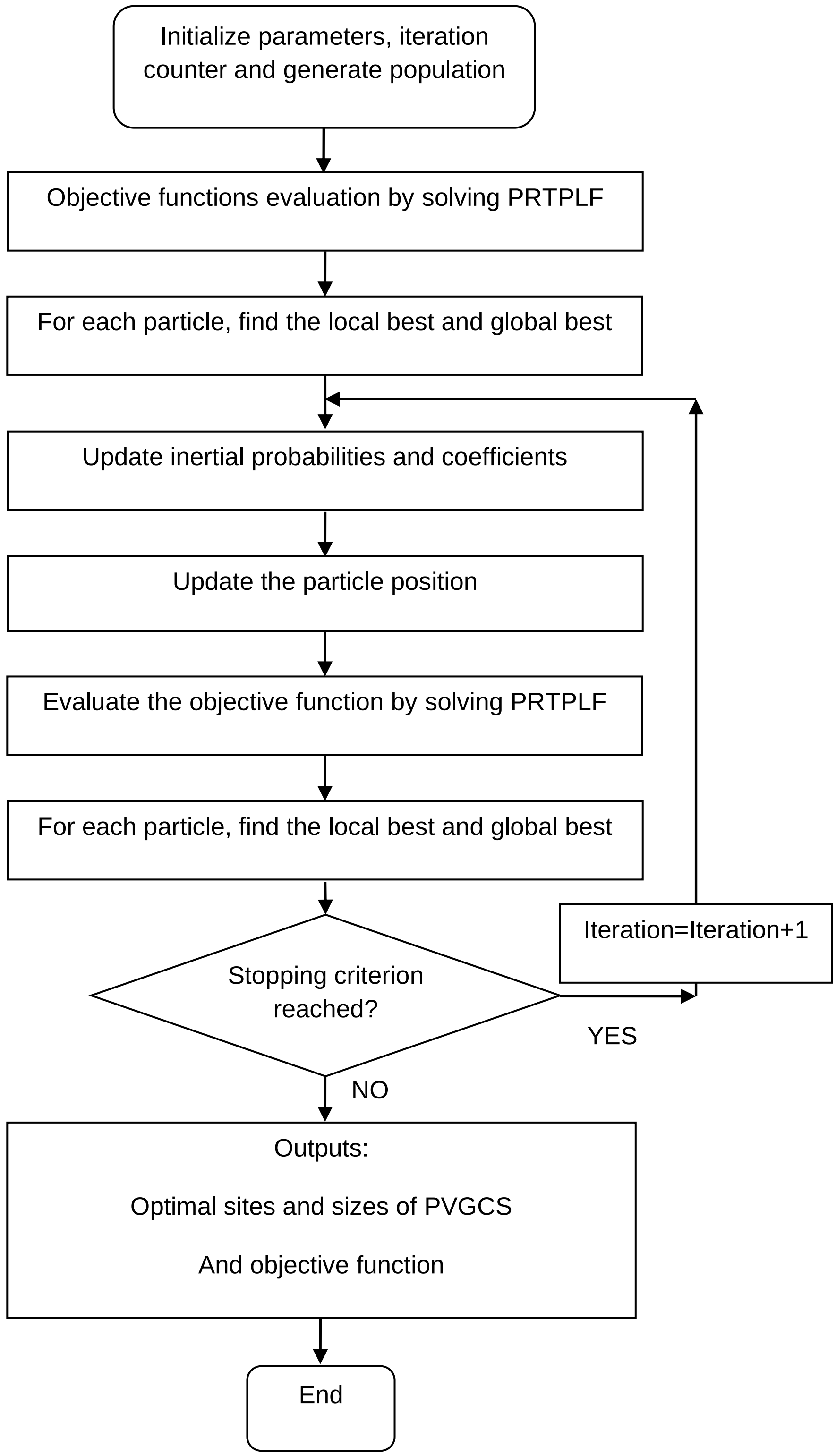

Fig. 4. Flow-chart of the proposed method JFPSO- PRTPLF.

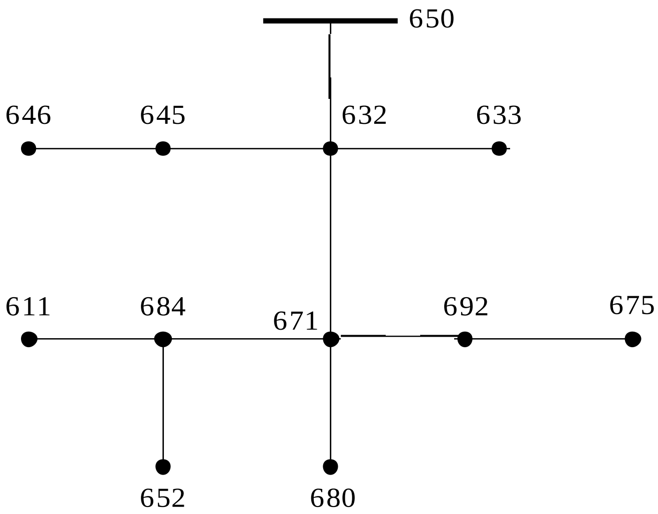

Fig. 5. System used in case study.

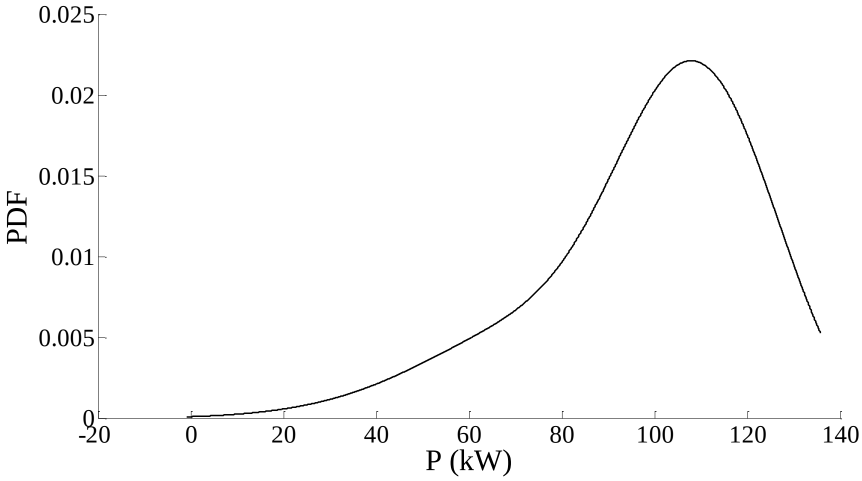

Fig. 6. PDF of a generator.

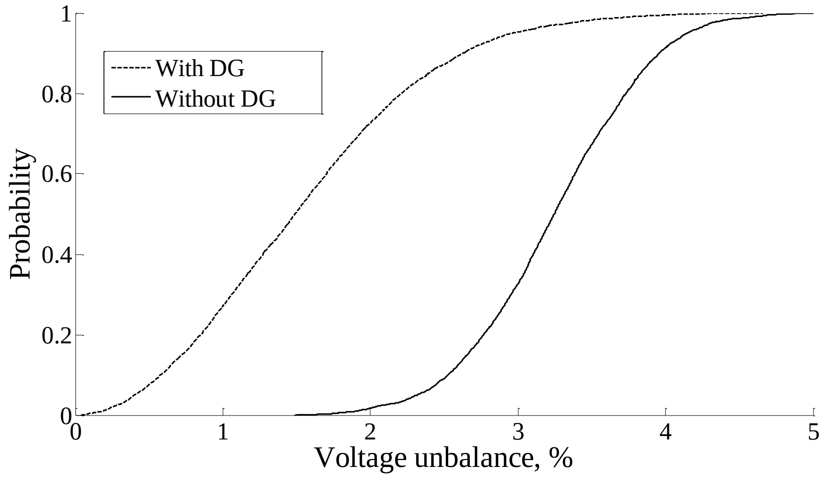

Fig. 7. CDF of the voltage unbalance at node 633.

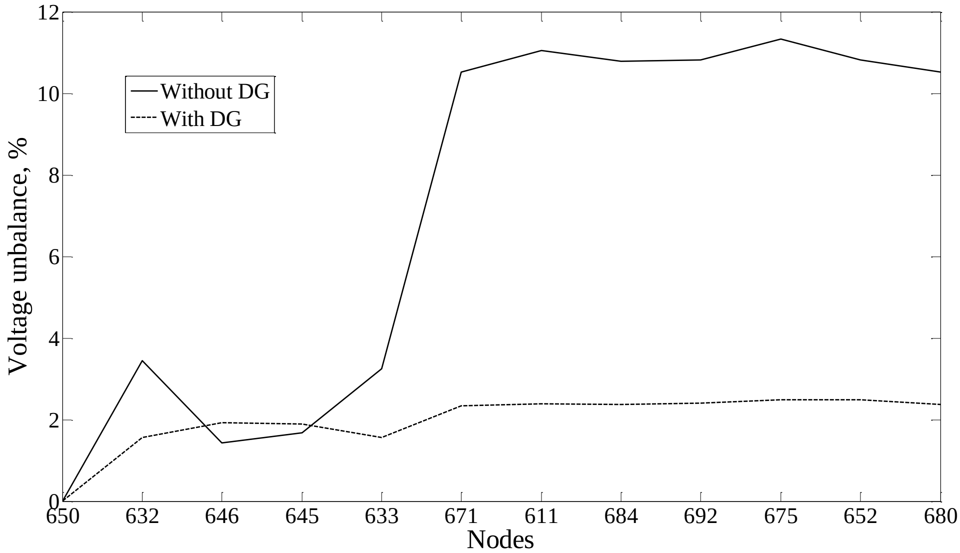

Fig. 8.Voltages unbalance profiles.

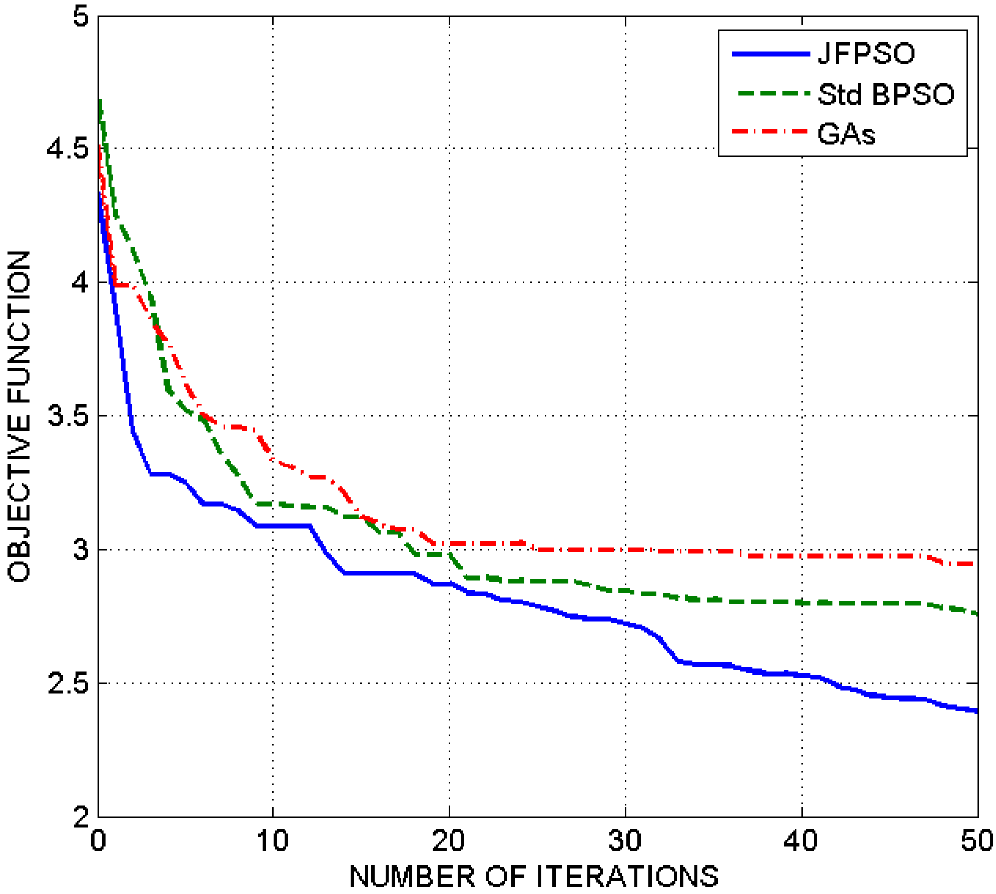

Fig. 9. Convergence curves of the used algorithms.